Journal of Hazardous Materials 475 (2024) 134853

Contents lists available at ScienceDirect

Journal of Hazardous Materials

journal homepage: www.elsevier.com/locate/jhazmat

Research Article

Breaking barriers in passive sampling: The potential of PTFE membranes in the monitoring of hydrophilic micropollutants

Naomi Reymond [a,*], Nicolas Estoppey [b,*], Céline Weyermann [a], Vick Glanzmann [a]

[a] School of Criminal Justice, University of Lausanne, Batochime building, Lausanne 1015, Switzerland
[b] Norwegian Geotechnical Institute (NGI), P.O. Box 3930, Ullevål Stadion, Oslo N-0806, Norway

HIGHLIGHTS

- First use of PTFE membranes in Chemcatcher-like samplers.
- PTFE membranes accumulate micropollutants 2000 times less than sorbent.
- R_S with PTFE membranes are 2.5 times higher than with PES membranes.
- Thick PTFE membranes enable R_S prediction without calibration experiments.

GRAPHICAL ABSTRACT

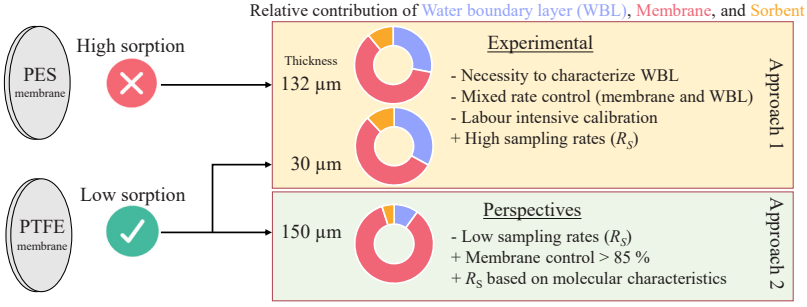

ARTICLE INFO

Keywords:
Calibration
Hydrodynamics
Environmental chemistry
Water quality monitoring
Membrane properties

ABSTRACT

Passive samplers are key tools to sample hydrophilic micropollutants in water. Two main approaches address the influence of hydrodynamics: (1) determining site-specific sampling rate (R_S) by characterizing k_w, the mass transfer coefficient of the water-boundary layer (WBL), and (2) reducing WBL impact using a diffusive material to control the uptake. The first requires calibration data and the second has only been achieved using fragile diffusive material. This study assesses the transfer of hydrophilic contaminants through polytetrafluoroethylene (PTFE; 30 µm thick), a new membrane material with lower sorption than commonly used polyethersulfone (PES). Combined for the first time in a Chemcatcher-like configuration, we calibrated the modified samplers for 44 micropollutants to provide R_S – k_w relationships for in-situ R_S determination (approach 1). Micropollutants accumulated over 2000 times more on the sorbent than on PTFE. PTFE-based R_S (0.027 to 0.300 L day^{-1}) were 2.5 higher than previously reported with PES. Membrane property measurements (porosity, tortuosity) indicated that accumulation is primarily controlled by the membrane. Extrapolation indicated that using thicker PTFE membranes ($\geq$ 100 µm) would shift uptake control entirely to the membrane in river conditions (approach 2). This finding could enable R_S prediction based on contaminants properties, thus representing a significant advancement in passive sampling.

* Corresponding authors.
E-mail addresses: naomi.reymond@unil.ch (N. Reymond), nicolas.estoppey@ngi.no (N. Estoppey).

https://doi.org/10.1016/j.jhazmat.2024.134853
Received 22 March 2024; Received in revised form 22 May 2024; Accepted 6 June 2024
Available online 7 June 2024

1. Introduction

Hydrophilic micropollutants, including pharmaceuticals and pesticides, are frequently detected in surface waters and their presence poses a significant risk to human health and the environment [1]. However, monitoring these compounds in water is challenging due to their low concentrations and high variability in time and space [2]. Active automated sampling is usually used, but passive sampling represents a promising alternative for large-scale monitoring of micropollutants, as it does not require power supply and provides time-integrated representative data on the freely dissolved fraction of contaminants [3]. The Chemcatcher is a widely used type of passive sampler (PS) for hydrophilic micropollutant monitoring. It is composed of a solid phase extraction disk (sorbent) and can be covered by a membrane, depending on the objectives of its implementation [4].

The sampling rate (R_S) of passive samplers – i.e., the volume of water sampled per time unit – is a key parameter to calculate the aqueous time-weighted average (TWA) concentration of contaminants from the amounts accumulated in the samplers. The main challenge when using integrative passive samplers is related to the fact that R_S is compound-specific and depends also on environmental factors, especially hydrodynamics [5]. For Chemcatchers, the uptake of micropollutants can be partially or fully controlled by the kinetics in the water boundary layer (WBL, which is a layer at the interface between the water and the sampler), the membrane, and the sorbent [6–10]. The thickness of the WBL, and therefore the resistance to mass transfer, decreases as the water velocity increases [11,12]. Control from the WBL means that R_S needs to be determined under field-relevant conditions to account for resistance changes. If the membrane (or another diffusive layer) controls the uptake, the resistance in the WBL becomes negligible and thus the influence of hydrodynamics can theoretically be eliminated. Sorbent control should be minimal so that the R_S is time-independent.

One approach is to calibrate the PS under controlled mass transfer coefficients of the WBL (k_w), a parameter that allows characterization of the hydrodynamic conditions [13,14], and then to measure k_w in the field to determine the in-situ R_S (approach 1). With this approach, the R_S are adjusted to account for the hydrodynamic conditions. Successful implementation has been demonstrated using Chemcatcher-like PS with styrenedivinylbenzene – reverse phase sulfonate (SDB-RPS, hereinafter referred to as SDB) sorbent covered by polyethersulfone (PES) membranes [15,16]. The drawback of this approach is the labour intensive calibration experiment that needs to be repeated for every contaminant added to the method. Additionally, the use of PES membranes should be avoided because the less hydrophilic compounds accumulate more in this layer than on the sorbent [15,17–19], preventing a good description of the uptake and potentially leading to biased interpretation of results [20,21].

Another approach to deal with the impact of hydrodynamics on the uptake of passive samplers is to cover the sorbent with a (thick) diffusive material that controls the uptake, thus allowing it to minimize the relative resistance in the WBL (approach 2). This allows for the determination of R_S from compound properties, independently of the hydrodynamics and without calibration experiments. This strategy is exploited in the organic-diffusive gradients in thin-films (o-DGT) samplers that rely on a very thick diffusive gel such as agarose gel [22]. These samplers are much less influenced by hydrodynamics than Chemcatchers. However, challenges with o-DGT include (i) small sampling surface area (i.e., only 3.14 cm^2 versus 15.2 cm^2 for Chemcatchers) and thus small sampling rates [23,24], and (ii) depletion and biodegradation of diffusion gels (i.e., uncertainties in TWA concentration) [25]. Several recently proposed designs of o-DGT with larger surface areas were shown to improve the sensitivity [26–30] but do not solve the challenge of the fragile diffusion gels, thus requiring to cover this layer with an additional protective layer, typically a PES membrane – which should be avoided when possible [28,29,31]. The use of a thick diffusive layer to control the uptake has not yet been tested with Chemcatcher PS.

In this study, we mechanistically assessed the transfer of hydrophilic contaminants through polytetrafluoroethylene (PTFE) membranes. This material could be a good alternative to PES, because little to no sorption occurs in PTFE [7,19,21,32,33]. The performance of this membrane when combined with Chemcatcher-like PS with SDB sorbent in controlled k_w (approach 1) was tested, and the conditions in which PTFE membranes could control the uptake are discussed (approach 2). The specific aims of this study were to (i) calibrate the passive samplers at four different flow velocities - under controlled k_w - to evaluate the impact of hydrodynamic conditions on the uptake of micropollutants, (ii) provide calibration data that can be used to determine in-situ R_S based on field measurements of k_w, (iii) compare the results obtained with PTFE membranes to previously published results obtained with PES membranes for the same compounds, (iv) acquire data on key membrane properties (porosity, and tortuosity) to characterize the sorption and mechanistically describe the transfer processes through the PTFE and PES membranes, (v) determine the relative resistance of each phase (WBL, membrane and sorbent) to determine in which conditions the uptake is controlled by the membrane, and would allow for R_S predictions based on contaminants properties. The novelty of this study lies in the use of a PTFE membrane in a Chemcatcher-like hydrophilic sampler, the data on porosity and tortuosity of the membranes, the determination of the relative resistance of each phase (WBL, membrane and sorbent), and the extrapolation of results to predict R_S without calibration experiments.

2. Materials and methods

2.1. Calibration experiment

2.1.1. Initial setup

Calibration of the samplers was conducted in a 4-channel system [34]. Water from Lake Geneva was used and continuously refreshed with a complete renewal in 24 h. The pH and temperature were monitored (Multiline Multi 3620 IDS, WTW, USA) and set to remain constant at pH 8 and 11 °C. The water was continuously spiked with the compounds of interest (Table 1) to achieve a concentration of 0.8 µg L^{-1} using a peristaltic pump. The concentration of the analytes in water was monitored with an automated refrigerated sampler (ISCO 6712FR, Teledyne ISCO, USA) set to collect samples at a rate of 50 mL h^{-1}. These samples were then combined to form daily composite samples. After the initial spiking of the analytes (day 1), the system was given time to equilibrate until the first samplers were deployed (day 4) (Supporting Information (SI) 1). Between days 20 – 23, some issues were encountered with the tubing of the peristaltic pump and the aqueous concentrations decreased below the set 0.8 µg L^{-1} for all compounds. At day 24, the tubing was replaced and the desired aqueous concentrations were reached again until the end of the experiment (day 32).

Constant water flow velocities were set at 5, 12, 20, and 40 cm s^{-1} for channels 1 to 4 (C1-C4), respectively. Alabaster-based mass transfer coefficients k_w were measured to characterize hydrodynamics at the surface of the samplers [13,15,34]. This was done by determining the mass loss of alabaster plates after exposure in the channels (1 – 5 h in the channels).

Solid-phase extraction disks (47 mm) with SDB sorbent (Affinisep, France) and hydrophilic PTFE membranes (Omnipore, 47 mm, 30 µm thick, 0.1 µm pores) (Merck, Germany) were conditioned successively in methanol (30 min) and ultra-pure water (> 30 min) under gentle stirring [35]. SDB disks and PTFE membranes were sandwiched between the plates of a custom housing in stainless steel with an exposed area of 12.6 cm^2 [16]. One housing has two positions and can therefore hold two duplicates (SI 2). Samplers were deployed in the 4 channels at mid-height and parallel to the flow for 7 different exposure durations (1, 2, 4, 8, 12, 15, and 21 days). After exposure, excess water was removed from the sampler with aluminium sheets, and SDB disks and PTFE membranes were placed in individual amber glass vials. In the

Table 1
Compounds of interest with CAS number (No), molecular weight (MW), and logK_{OW}.

Compound	CAS No	MW	logK_{OW}[a]
2,4-D	94-75-7	221.04	-0.8 (−5.4)
5MethylBenzotriazole	136-85-6	133.15	1.61
Atrazine	1912-24-9	215.68	2.6
Azoxystrobin	131860-33-8	403.39	2.5
Bentazon	25057-89-0	240.28	2.34
Boscalid	188425-85-6	343.21	3
Caffeine	58-08-2	194.19	-0.07
Carbamazepine	298-46-4	236.27	2.45
Carbendazim	10605-21-7	191.19	1.52
Chloridazon	1698-60-8	221.64	1.14
Chlorotoluron	15545-48-9	212.68	2.41
Cyproconazol	94361-06-5	291.78	3.1
Cyprodinil	121552-61-2	225.29	4
DEET	134-62-3	191.27	2.02
Diclofenac (acid)	15307-86-5	296.1	4.51 (0.66)
Dimethachlor	50563-36-5	255.74	2.17
Dimethenamid	87674-68-8	275.79	2.2
Dimethoate	60-51-5	229.26	0.8
Diuron	330-54-1	233.09	2.68
Ethofumesate	26225-79-6	286.34	2.7
Flufenacet	142459-58-3	363.33	3.2
Foramsulfuron	173159-57-4	452.44	-0.8
Imidacloprid	105827-78-9	255.66	0.6
Iprovalicarb	140923-17-7	320.43	3.2
Isoproturon	34123-59-6	206.28	2.87
Linuron	330-5-2	249.09	3.2
MCPA	94-74-6	200.62	-0.8 (−5.1)
Metalaxyl-M	70630-17-0	279.33	1.8
Metamitron	41394-05-2	202.24	0.83
Metazachlor	67129-08-2	277.75	2.13
Metolachlor	51218-45-2	283.79	3.12
Metribuzin	21087-64-9	214.29	1.7
Napropamid	15299-99-7	271.35	3.36
Nicosulfuron	111991-09-4	410.41	0.6 (−2.6)
Pirimicarb	23103-98-2	238.29	1.7
Propamocarb	24579-73-5	188.27	0.8 (−0.7)
Propyzamid	23950-58-5	256.12	3.43
Pyrimethanil	53112-28-0	199.26	2.8
Sulfamethoxazole	723-46-6	253.28	0.89
Tebuconazol	107534-96-3	307.82	3.7
Terbuthylazine	5915-41-3	229.71	3.21
Terbutryn	886-50-0	241.36	3.74
Thiacloprid	111988-49-9	252.72	1.3
Thiamethoxam	153719-23-4	291.71	-0.1

[a] Partition coefficients in brackets are normalized to the fraction of the neutral species at pH 8 using D_{OW} (pH 8)= $1/(1+10^{(8\text{-pKa})})K_{OW}$.

laboratory, 7 mL of acetone were added to each vial before freezing (- 24 °C) them until extraction.

2.1.2. Extraction and chemical analysis

All samplers were thawed for 30 min before extraction. SDB disks and PTFE membranes were then shaken for 30 min (rotary shaker, 30 rpm). The extract was transferred to another vial, and a second extraction took place with 7 mL of methanol (rotary shaker, 30 rpm, 30 min), before combining both extracts (14 mL in total). Chemical analysis was achieved by LC-MS/MS (AB Sciex QTRAP 6500 +) with a Phenomenex Luna Omega column (C18, 150 mm × 2.1 mm×1.6 µm, 100 Å). Composite water samples from the channel system were combined to obtain 24 h-composite samples and were analysed like the SDB and PTFE samples. Additional details on LC-MS/MS methods can be found in Reymond et al. [16].

2.1.3. Data treatment

The R_S (L day^{-1}) were determined using the sampling rate model [36]:

$$V_e = mK_{SW}\left(1-\exp\left(-\frac{R_s t}{mK_{SW}}\right)\right) \quad (1)$$

with V_e the equivalent sampled volume (L), m the mass of the SDB disk (kg), K_{SW} the sampler-water partition coefficient (L kg^{-1}), and t the time (day). R_S were calculated on day 14 (which corresponds to a typical deployment time) by dividing V_e by t.

For each target compound, alabaster-based k_w were adapted to the corresponding organic contaminant $k_{w,org}$ (dm day^{-1}), using the diffusion coefficients in water of the contaminant $D_{w,org}$ (m^2 s^{-1}), calculated from McGowan volumes [37]. $D_{w,org}$ were adjusted to the experimental temperature T_{exp} [38] using the dynamic viscosity η (Pa s).

$$D_{w,Texp} = D_{w,25°C}\left(\frac{\eta_{T=25°C}}{\eta_{T_{exp}}}\right)^{1.14} \quad (2)$$

$$k_{w,org} = k_{w,alabaster}\left(\frac{D_{w,org}}{D_{w,alabaster}}\right)^{2/3} \quad (3)$$

Then, the four R_S from the four channels were plotted against the $k_{w,org}$, and fitted to 2 models for mixed rate control by the membrane and the WBL (MRC model - Eq. 4, and adapted MRC model - Eq. 5) [14,15]:

$$\frac{1}{R_S} = \frac{1}{Ak_w} + \frac{1}{R_{S,MAX}} \quad (4)$$

$$\frac{1}{R_S} = \frac{a}{Ak_w} + \frac{1}{R_{S,MAX}} \quad (5)$$

where A (dm^2) represents the sampler's area, and a and $R_{S,MAX}$ (L day^{-1}) are the adjustable parameters.

2.2. Porosity and tortuosity

Mercury intrusion porosimetry (MIP) was used to determine the pore size diameters and the porosity (φ) of PES membranes (47 mm diameter, 132 µm thick, 0.1 µm pores (PALL Science, USA)) and the above-mentioned PTFE membranes (same pore size as PES membranes, i.e., 0.1 µm, according to the manufacturer). Mercury penetrates the open pores under increasing pressure. The intrusion volume of mercury is measured and used to calculate the pore size using Washburn's equation (Eq. 6) [39]. Porosity (%) is the ratio of the total pore volume to the bulk volume of the material.

$$P = -\frac{2\gamma\cos\theta}{r} \quad (6)$$

with P the applied pressure (Pa), γ the surface tension (N m^{-1}), θ the contact angle (°), and r the capillary radius (m). θ was unknown and set at 140°.

The group porosity/tortuosity^2 (φ/τ^2) of PES and PTFE membranes was measured in C3 of the channel system using the dissolution of alabaster plates [13] with (Eq. 7) and without (Eq. 8) conditioned membranes:

$$\Delta m_1 = R_{S,o}C^* t \quad (7)$$

$$\Delta m_2 = R_{S,w}C^* t \quad (8)$$

with Δm_1 and Δm_2 (g) the mass loss of alabaster with and without membrane respectively, $R_{S,o}$ the overall R_S for mixed rate control by the membrane and the WBL, $R_{S,w}$ the R_S for full WBL control, and C^* the solubility of alabaster in the exposure water (g L^{-1}).

The R_S for full membrane-controlled kinetics, $R_{S,m}$, can be found from experimentally measured $R_{S,o}$ and $R_{S,w}$ using Eq. (9) [40]:

$$\frac{1}{R_{S,o}} = \frac{1}{R_{S,w}} + \frac{1}{R_{S,m}} \quad (9)$$

The group φ/τ^2 can be calculated using Eq. (10), with d_m the membrane's thickness (µm) given by the manufacturer [41]. Finally, because porosity is known (MIP experiment), tortuosity can be deduced from the

φ/τ^2 value. Tortuosity can be defined as the length of the diffusion path divided by the thickness of the membrane [40].

$$R_{S,m} = \frac{\varphi D_w}{\tau^2 d_m} A \quad (10)$$

3. Results and discussion

3.1. Conditions in the channel-system

Hydrodynamic conditions, characterized by k_w with the alabaster plates before and after spiking, were: 2.56 μm s^{-1} (C1), 5.18 μm s^{-1} (C2), 8.63 μm s^{-1} (C3), and 12.12 μm s^{-1} (C4). For most analytes, water concentrations in the channel system remained stable (between 206.3 and 882.6 ng L^{-1} depending on the analyte, RSD $\leq$ 20 %) during the calibration experiment (days 4 – 32). For dimethoate, ethofumesate, flufenacet, foramsulfuron, metazachlor, nicosulfuron, and pyrimethanil, the concentration was stable (RSD $\leq$ 20 %) except for the period during which there was an issue with the peristaltic pump (days 20 – 23). The higher RSD when taking days 20 – 23 into account is not a problem for the calibration experiment because the accumulated mass on the sampler is normalised by the average water concentration during the exposure period (when determining V_e).

3.2. Sampling rates and relationships with mass transfer coefficients of the water boundary layer

The accumulated mass in the SDB disks is expected to increase with time and flow velocity (up to the maximum sampling rate, $R_{S,MAX}$, attained at high velocities) as long as the uptake is (at least, partially) controlled by the WBL [10,42,43]. Apart from short exposure times (< 4 days) in the slowest channel (C1), all analytes were detected in the SDB disks. The accumulated mass after 15 days (which corresponds to the usual deployment time for Chemcatchers) ranged from 117.7 ng (nicosulfuron, C1) to 2515.8 ng (dimethachlor, C3). The expected increase between C3 and C4 has not been observed, probably because hydrodynamic conditions in C3 and C4 are close to $R_{S,MAX}$ conditions (see discussion below). Two different analyte behaviours were observed (Fig. 1, Table 2, SI 3). Initially, the majority (25) of analytes displayed a linear uptake over the 21-day experiment (given by Eq. (11), the half-time to equilibrium $t_{1/2} > 21$ days [44]) in all four channels, suggesting time-integrative accumulation with constant R_S for these compounds. Some additional compounds showed a linear uptake over 21 days but only in the slower channels (1 compound in C1 – C2 – C3, 1 in C1 – C2, 3 in C1). One compound (iprovalicarb) was linear for C2 – C3 – C4 but not C1, which cannot be explained.

$$t_{1/2} = \frac{mK_{SW}}{R_S} \ln(2) \quad (11)$$

The second behaviour (13 compounds in C1 to C4) exhibited a curvilinear uptake already for shorter periods, eventually reaching a plateau with longer accumulation times, indicating sorbent-controlled uptake kinetics to some degree, which also implies that the sorbent does not act as an infinite sink [6]. This is corroborated by the small modelled mK_{SW} values observed for these compounds, signifying an increase in sorbent resistance over time as the concentration gradient diminishes within the sorbent, eventually reaching a state of partial equilibrium. To explain this behaviour, diffusion models may provide a better understanding than the sampling rate model. Diffusion models are based on the integration of Fick's second law and use the mathematical analysis of the concentration profiles within the sorbent to determine R_S [6]. The model from Booij [6] was applied to the 13 compounds exhibiting sorbent control and the results from both models were in very good agreement. However, because the complex diffusion model did not provide an added value for this dataset (SI 4), the following analyses are based solely on the sampling rate model.

The obtained R_S on day 14 range from 0.027 L day^{-1} for nicosulfuron (C1) to 0.247 L day^{-1} for dimethachlor (C3), with a median of 0.153 L day^{-1} (Table 2). Because micropollutants accumulated more in the SDB disks in C3 than in C4, R_S in C3 were slightly higher than in C4. This is probably due to hydrodynamic conditions being close to $R_{S,MAX}$ conditions (see discussion below) and can be associated with the experimental uncertainty.

To establish relationships between R_S and k_w, the MRC model (Eq. 4) and the adapted MRC model (Eq. 5) were tested. The parameters for both models are provided in Table 2. Both models effectively predict R_S based on k_w (Fig. 2). The data points from the calibration experiment are close to $R_{S,MAX}$, suggesting that hydrodynamic conditions have a minimal influence on R_S within the examined range. This explains why the increase in accumulated masses was not observed between C3 and C4, as well as why the R_S between C3 and C4 were similar. The adapted MRC model exhibits a slightly improved fit to the data when compared to the original MRC model, as indicated by the smaller sum of squared residuals (SSQ) values (median SSQ $5.0 \bullet 10^{-5}$ vs $9.9 \bullet 10^{-4}$, respectively) (Fig. 2). In this adapted model, the parameter a is introduced as an adjustable parameter in the equation. Except for 3 compounds, a values were below 1 (median $a = 0.506$), which may be due to reduced resistance in the WBL ($\frac{1}{Ak_w}$) when the flow passes through the membrane. The adapted MRC model was proposed because some R_S obtained at high water velocities exceeded $R_{S,MAX}$ [15]. Even though they obtained better fittings, there is no mechanistic basis for the additional a parameter in the model. In the present study, none of the R_S obtained in the fastest channels exceeded $R_{S,MAX}$, and the SSQ were acceptable for

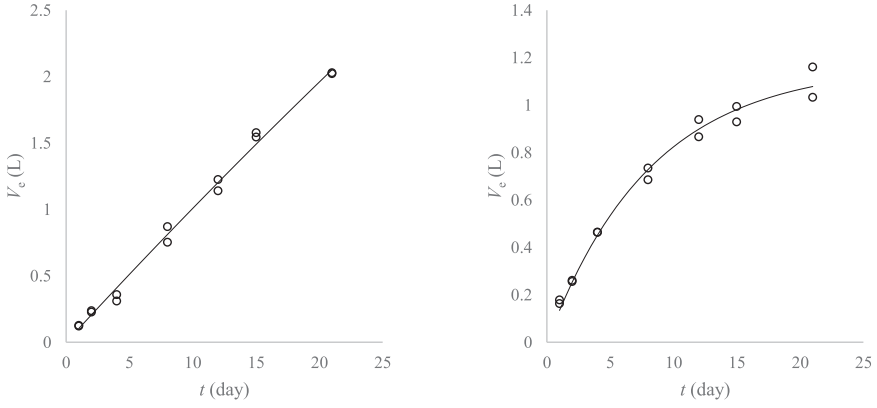

Fig. 1. Two different types of compound behaviours. Left: linear uptake for diclofenac acid in channel 1 (5 cm s^{-1}), Right: curvilinear uptake then plateau for bentazon in channel 4 (40 cm s^{-1}).

Table 2
Sampling rates R_S (L day^{-1}) and parameters for k_w-R_S relationships with the MRC model and the adapted MRC model (Eqs. 4 and 5). ^{CL} indicates curvilinear uptake ($t_{1/2}$ <21 days) in the channel, otherwise uptake is linear. Water flow velocities are 5, 12, 20, and 40 cm s^{-1} in C1-C4, respectively.

	Sampling rates				MRC model	Adapted MRC model	
	C1	C2	C3	C4	$R_{S,MAX}$	a	$R_{S,MAX}$
2,4-D	0.049^{CL}	0.051^{CL}	0.054^{CL}	0.054^{CL}	0.059	0.639	0.057
5MethylBenzotriazole	0.103^{CL}	0.118^{CL}	0.134^{CL}	0.133^{CL}	0.156	0.773	0.150
Atrazine	0.138	0.155^{CL}	0.179^{CL}	0.175^{CL}	0.235	0.456	0.196
Azoxystrobin	0.121	0.140	0.169	0.163	0.232	0.502	0.192
Bentazon	0.063^{CL}	0.064^{CL}	0.069^{CL}	0.068^{CL}	0.077	0.395	0.071
Boscalid	0.132	0.151	0.184	0.179	0.248	0.549	0.211
Caffeine	0.082^{CL}	0.088^{CL}	0.095^{CL}	0.093^{CL}	0.109	0.445	0.099
Carbamazepine	0.141	0.162	0.192	0.187	0.260	0.495	0.216
Carbendazim	0.107^{CL}	0.122^{CL}	0.136^{CL}	0.134^{CL}	0.164	0.574	0.149
Chloridazon	0.140^{CL}	0.158^{CL}	0.185^{CL}	0.183^{CL}	0.244	0.508	0.208
Chlorotoluron	0.143	0.174	0.198	0.194	0.269	0.514	0.226
Cyproconazol	0.135	0.155	0.192	0.184	0.261	0.537	0.219
Cyprodinil	0.153^{CL}	0.181^{CL}	0.221^{CL}	0.210^{CL}	0.308	0.510	0.252
DEET	0.133^{CL}	0.152^{CL}	0.168^{CL}	0.165^{CL}	0.222	0.409	0.183
Diclofenac (acid)	0.100	0.114	0.134	0.129	0.163	0.633	0.149
Dimethachlor	0.174	0.197	0.247^{CL}	0.220^{CL}	0.355	0.380	0.264
Dimethenamid	0.151	0.171	0.207	0.199	0.292	0.444	0.231
Dimethoate	0.126	0.142^{CL}	0.158^{CL}	0.159^{CL}	0.205	0.464	0.175
Diuron	0.148	0.175	0.211	0.202	0.285	0.535	0.240
Ethofumesate	0.140	0.169	0.202	0.195	0.282	0.526	0.233
Flufenacet	0.145	0.162	0.209	0.195	0.285	0.526	0.236
Foramsulfuron	0.041^{CL}	0.046^{CL}	0.052^{CL}	0.051^{CL}	0.055	1.098	0.056
Imidacloprid	0.135	0.159	0.182	0.176^{CL}	0.241	0.487	0.203
Iprovalicarb	0.114^{CL}	0.139	0.173	0.158	0.215	0.684	0.196
Isoproturon	0.135	0.154	0.181	0.177	0.240	0.505	0.203
Linuron	0.157	0.180	0.225	0.215	0.311	0.536	0.258
MCPA	0.059^{CL}	0.062^{CL}	0.065^{CL}	0.065^{CL}	0.072	0.500	0.068
Metalaxyl-M	0.131	0.152	0.180	0.173	0.235	0.530	0.201
Metamitron	0.119	0.134^{CL}	0.149^{CL}	0.145^{CL}	0.186	0.460	0.161
Metazachlor	0.149	0.182	0.206	0.199	0.297	0.424	0.232
Metolachlor	0.143	0.166	0.200	0.192	0.283	0.466	0.226
Metribuzin	0.138	0.157	0.179	0.175	0.236	0.457	0.197
Napropamid	0.146	0.169	0.197	0.196	0.285	0.437	0.225
Nicosulfuron	0.027^{CL}	0.030^{CL}	0.032^{CL}	0.031^{CL}	0.033	1.164	0.034
Pirimicarb	0.136	0.159	0.187	0.181	0.252	0.500	0.210
Propamocarb	0.037	0.045	0.051	0.050	0.051	2.059	0.058
Propyzamid	0.136^{CL}	0.155^{CL}	0.173^{CL}	0.174^{CL}	0.235	0.421	0.193
Pyrimethanil	0.143	0.184	0.210	0.210	0.294	0.586	0.252
Sulfamethoxazole	0.053^{CL}	0.056^{CL}	0.058^{CL}	0.058^{CL}	0.064	0.413	0.060
Tebuconazol	0.129	0.150	0.189	0.180	0.258	0.574	0.219
Terbuthylazine	0.144	0.169	0.205	0.197	0.278	0.538	0.234
Terbutryn	0.140	0.166	0.200	0.190	0.272	0.519	0.226
Thiacloprid	0.151	0.179	0.210	0.205	0.290	0.503	0.240
Thiamethoxam	0.120^{CL}	0.132^{CL}	0.150^{CL}	0.146^{CL}	0.191	0.438	0.162

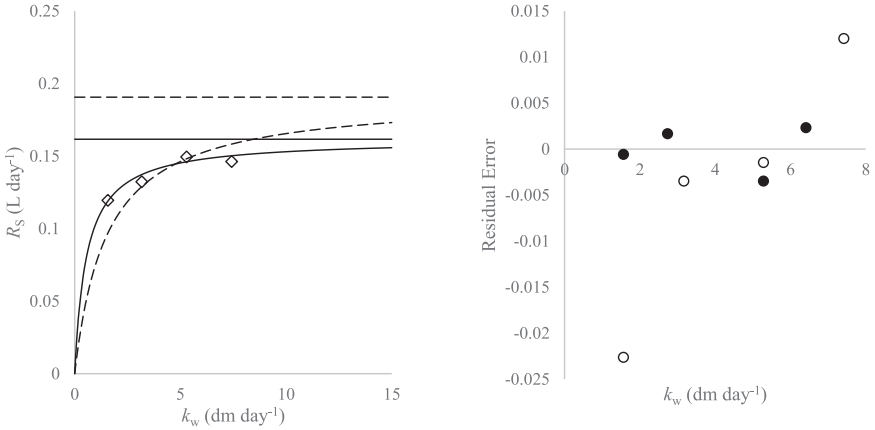

Fig. 2. (a) Left: examples of k_w-R_S relationships for thiamethoxam with the MRC model (dashed line) and adapted MRC model (solid line), horizontal lines are $R_{S,MAX}$, diamonds are data points from calibration experiment. (b) Right: residual errors for thiamethoxam with the MRC model (empty circles) and adapted MRC model (filled circles).

both models (max SSQ $< 4.3 \bullet 10^{-3}$), indicating that the use of the adapted MRC model may not be necessary for this PS design.

In this first approach, PS were calibrated under 4 controlled k_w to evaluate the impact of hydrodynamic conditions on the uptake of 44 micropollutants. This calibration provides data that can be used for PS with similar configurations (SDB disk, PTFE membrane) to determine in-situ based R_S if k_w is measured in the field, using Eq. (4). A silicone disk spiked with performance reference compounds (PRC) can be deployed simultaneously to measure k_w [34].

3.3. Accumulation in PTFE membranes

The role of the membrane is to protect the sorbent, to be selective of accumulated micropollutants, and to extend the kinetic regime [4]. The membrane should not be another layer into which compounds could accumulate because it might affect the interpretation of results [20,21]. No accumulation was observed in the PTFE membrane for 9 micropollutants exposed during 21 days. For the other compounds (35), the accumulation in the SDB disk exceeded that in the PTFE membrane by factors ranging from 52 to over 157'000 (average 2074 times more, median 700 times more). No correlation was found between the sorption onto the PTFE membrane and the physicochemical properties of the compounds (e.g., Pearson −0.34 for logK_{OW}, −0.18 for molecular weight). Since the accumulation is low, the advantages of employing PTFE as membrane material is confirmed, especially in regards to widely used PES membranes as they have shown strong accumulations [15, 17–19,32]. The reusability of the PTFE membranes should be evaluated, for example by comparing the properties of new and reused membranes with a diffusion cell [21]. This could help to reduce costs, given that this material is approximately three times more expensive than PES, and also lower the environmental impact of the sampler by limiting single-use materials.

3.4. Impact of membrane properties on contaminant transfer

Since PES membranes are more commonly used with Chemcatcher-like samplers, a comparison was made between R_S obtained with PTFE and PES membranes ($R_{S,PTFE}$ and $R_{S,PES}$, respectively). All the data for PES membranes is derived from a previous calibration experiment conducted by Glanzmann et al. [15] under comparable conditions (sampler configuration, pH, T, water velocity, exposure durations). R_S were calculated for a fixed $k_w = 10$ µm s^{-1}, using the parameters from the adapted MRC model (as it is more appropriate for PES membranes, and gives similar results to the MRC model for PFTE). $R_{S,PTFE}$ always exhibited higher values than $R_{S,PES}$ (Fig. 3, median $R_{S,PTFE} = 2.5R_{S,PES}$).

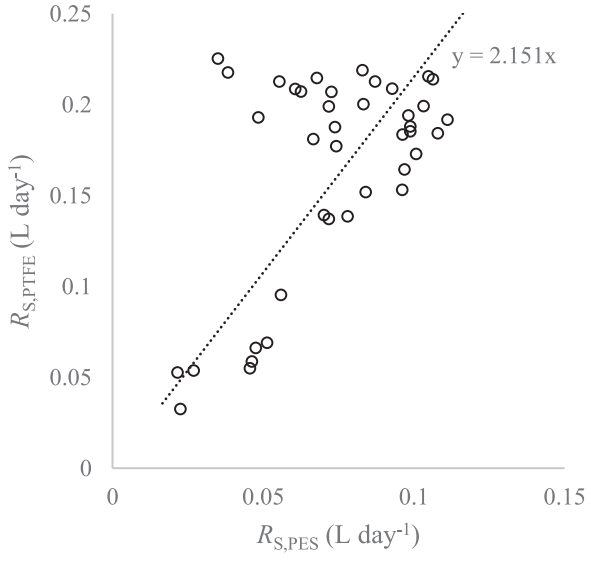

Fig. 3. Sampling rates R_S with PES and PTFE membranes calculated for $k_w = 10$ µm s^{-1} with the adapted MRC model. The dotted line is the trend line.

Physicochemical parameters of the membranes can explain these differences. First, the sorption by PTFE membranes is weaker compared to PES (as described in the previous section). If the analytes do not sorb on the membrane, they are more likely to accumulate on the sorbent, leading to higher R_S (as long as the equilibrium between the membrane and water is not reached). Secondly, assuming that transport resistance in the sorbent can be neglected and that transport in the membranes occurs only through the pore space, three parameters need to be discussed relating to Eq. (10) [13,21]. Combined as $\frac{d_m \tau^2}{\varphi}$, this group forms the effective thickness, which is a membrane property [40]. The PTFE membranes were thinner (d_m 30 µm) than PES membranes (d_m 132 µm), which shortens transfer duration through the membrane to the sorbent if other parameters are similar. With faster accumulation in the sorbent, the linear phase of the uptake is also reduced. The half-time to equilibrium was reached in under 14 days in C4 for 14 compounds with the PTFE membrane, compared to 3 compounds with the PES membrane. A thinner membrane also means that the uptake is more sensitive to flow variations because the membrane resistance becomes smaller while the relative resistance of the WBL increases at low flow velocities [45]. The use of a thin membrane contrasts with the development of other PS (e.g., o-DGT) where a thicker phase (e.g., diffusion layer) is used, making the resistance in this compartment higher than in the WBL (approach 2). The use of an additional silicone disk spiked with PRC (approach 1) is therefore of high interest with the sampler configuration from this study, as it allows for the consideration of hydrodynamic conditions [16]. Thinner membranes also increase the relative sorbent resistance, and thus the degree of sorbent-controlled kinetics. As discussed above, diffusion models should be used with compounds for which there is an important sorbent resistance. However, their use could be avoided by using thicker membranes [6].

Concerning the other parameters, and considering that transport only occurs through the pore space, the rate of transport within the membrane is increased by a larger porosity and less tortuous diffusion paths [40]. Using the porosity from MIP analyses (Table 3) and the experiments from the channel system ($\varphi/\tau^2_{PES} = 0.255$ and $\varphi/\tau^2_{PTFE} = 0.076$), tortuosity was calculated: $\tau_{PES} = 1.53$ and $\tau_{PTFE} = 1.84$. Furthermore, pore size can also impact transport processes [44,46]. Despite both membrane types being reported with a size of 0.1 µm by manufacturers, MIP analyses revealed distinct pore size distributions (Table 3). Notably, PTFE exhibited a higher prevalence of smaller pores. Smaller pores can hinder the diffusion of analytes through the membrane, and additional experiments are required to better understand this parameter.

Overall, the acquired data on membrane properties allowed us to characterise the sorption and to mechanistically describe the transfer processes through both types of material. Although PTFE membranes allow easier transport due to their lower sorption and thinner structure, porosity, tortuosity, and pore size were shown to also play a crucial role, affecting transport differently than in PES membranes.

Table 3
Results from MIP analyses for PES and PTFE membranes.

	Porosity[a] [%]	Average pore diameter[b] [nm]	Median pore diameter[b] [nm]
PES	60	112	246
PTFE	26	14	116

[a] Pore diameter range between 10 and 100'000 nm
[b] Range between 3 and 100'000 nm.

3.5. Resistance to mass transfer and relative contributions of each phase

The resistances to mass transfer ($1/R_S$) of the different phases (WBL, PES or PTFE membrane, and sorbent) were calculated to estimate their relative contributions in all four channels (between 2.56 µm s^{-1} and 12.12 µm s^{-1}). $R_{S,o}$ was determined at the corresponding k_w using eq. (4) and $R_{S,MAX}$ from Table 2 for the PS with the PTFE membrane. The same method was used to determine $R_{S,o}$ for PS with a PES membrane, using parameters from Glanzmann et al. [15]. $R_{S,w}$, and $R_{S,m}$ were determined from Eqs. (8) and (9), respectively, and $R_{S,SDB}$ was obtained with Eq. (12). $R_{S,SDB}$ is supposed to be the same for all PS using the same sorbent, because the accumulation on the sorbent is independent from the other layers. To account for the uncertainties associated with the method, the average $R_{S,SDB}$ was used (4 channels, 2 types of membranes).

$$\frac{1}{R_{S,o}} = \frac{1}{R_{S,w}} + \frac{1}{R_{S,m}} + \frac{1}{R_{S,SDB}} \quad (12)$$

Results show that in all cases, the membrane is the main contributor to resistance to mass transfer (Fig. 4). WBL control is considerable in the slowest channels (C1-C2) for both PES and PTFE membranes. As WBL control decreases with increasing water velocity, the resistance in the WBL becomes negligible (< 15 %) above 20 cm s^{-1}, as shown in previous studies [16,47]. The relative contribution of the sorbent is higher with PTFE than with PES membranes (14 % and 11 % on average, respectively). Considering the slowest channel (C1) sorbent resistance ($1/R_{S,SDB}$) was negative for 20 compounds. This indicates mixed rate control, primarily by the PTFE or PES membrane (63 % and 68 % respectively) and to a lesser extent by the WBL (37 % and 32 %, respectively). For 24 compounds, sorbent resistance was positive, contributing on average to 22 % (PTFE) and 20 % (PES) of the relative resistance (49 % and 54 % for the PTFE and PES membranes, 29 % and 26 % respectively for the WBL).

Extrapolation of the results (estimation of $R_{S,m}$ using Eq. 10) shows that employing a thicker PTFE membrane with a similar φ/τ^2 group would shift uptake toward full membrane control for all studied compounds (approach 2). Membrane control (> 85 %) would be achieved using a 100 µm thick membrane above 10 cm s^{-1} (k_w=5.14 µm s^{-1}), and using a 150 µm thick membrane for slower velocities (5 cm s^{-1}, k_w=2.56 µm s^{-1}). This result implies the ability to determine R_S for any hydrophilic organic compound without time-intensive calibration experiments if D_w is known, as per Eq. (10), at least within the studied hydrodynamic conditions. With a 100 µm thick PTFE membrane, R_S would range between 0.021 and 0.042 L day^{-1} for the studied compounds (one third smaller for 150 µm membranes). The estimated R_S are on average 6x smaller than the ones obtained for 30 µm membranes and within the same order of magnitude of R_S obtained with o-DGT (0.006–0.132 L day^{-1} for an upscaled PS [48], 0.009–0.016 L day^{-1} [23], 0.011 L day^{-1} for sulfamethoxazole [49]). If needed, the exposed area could be increased to improve the sensitivity of the sampler (e.g., the custom housing shown in SI2 can hold 2 samplers, sorbent and membranes with a diameter of 90 mm are commercially available).

In summary, the relative resistance of each phase was determined for PES and PTFE membranes, showing that in most cases the membrane is the main contributor in river-like conditions. Estimations showed that using thicker PTFE membranes could solve current issues encountered with the uptake of micropollutants on hydrophilic passive samplers by i) removing the need to characterise the WBL using a diffusion material that will control the uptake (similarly to o-DGT), ii) enabling easy R_S determination from D_w – a compound property, and iii) replacing PES membranes on which compounds accumulated strongly.

CRediT authorship contribution statement

Nicolas Estoppey: Writing – review & editing, Methodology, Conceptualization. **Céline Weyermann:** Writing – review & editing, Supervision, Conceptualization. **Vick Glanzmann:** Writing – review & editing, Supervision, Methodology, Investigation, Conceptualization. **Naomi Reymond:** Writing – original draft, Visualization, Methodology, Investigation, Formal analysis, Data curation, Conceptualization.

Environmental Implications

Hydrophilic micropollutants, such as pesticides, pharmaceuticals, and industrial compounds, contaminate surface waters worldwide. Their presence poses a significant risk to human health and the environment, making their monitoring crucial for environmental protection. Passive samplers are valuable tools for assessing the concentration of these contaminants in water. In this study, a Chemcatcher-like sampler was modified with new membrane material with little sorption affinity to micropollutants to enhance the monitoring accuracy of data by considering the hydrodynamic conditions. Results suggest that calibrations may not be necessary anymore, allowing for easy sampling of new contaminants.

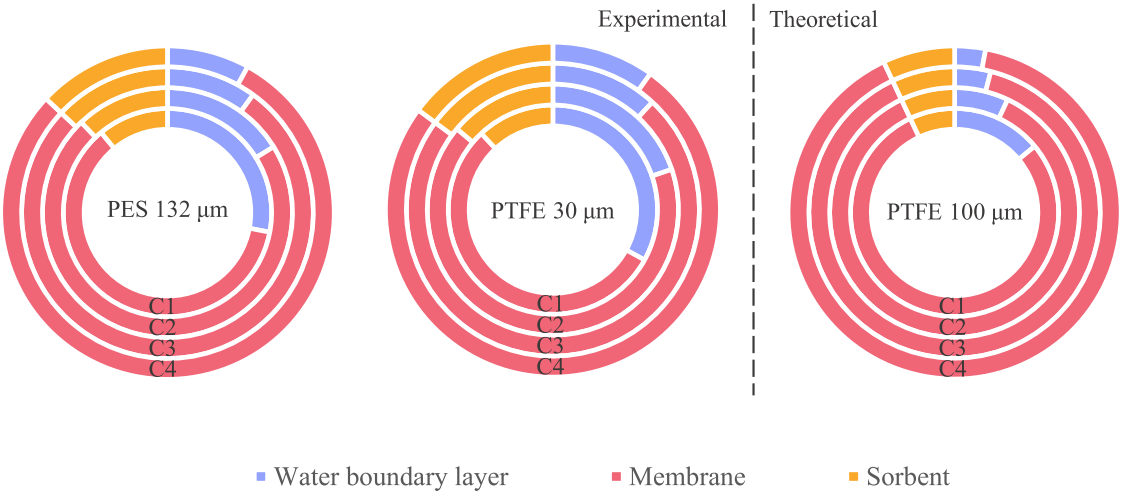

Fig. 4. Pie charts of the relative contributions of the WBL, the membrane, and the sorbent to resistance to mass transfer for 3 different membranes. Each circle shows contributions in a different channel (C1 (5 cm s^{-1}): k_w =2.56 µm s^{-1}, C2 (12 cm s^{-1}): k_w =5.18 µm s^{-1}, C3 (20 cm s^{-1}): k_w =8.63 µm s^{-1}, C4 (40 cm s^{-1}): k_w =12.12 µm s^{-1}).

Declaration of Competing Interest

The authors declare that they have no known competing financial interests or personal relationships that could have appeared to influence the work reported in this paper.

Data Availability

Data will be made available on request.

Acknowledgements

The authors would like to thank Kees Booij from PaSOC for the discussions around uptake models. Authors would also thank the Laboratory of Construction Materials at the Swiss Federal Institute of Technology in Lausanne, in particular Jean Dias Rego and Lionel Sofia, for the mercury intrusion porosimetry analyses.

Appendix A. Supporting information

Supplementary data associated with this article can be found in the online version at doi:10.1016/j.jhazmat.2024.134853.

References

[1] Schwarzenbach, R.P., Egli, T., Hofstetter, T.B., von Gunten, U., Wehrli, B., 2010. Global water pollution and human health. Annu Rev Environ Resour 35 (1), 109–136. https://doi.org/10.1146/annurev-environ-100809-125342.

[2] Vrana, B., Allan, I.J., Greenwood, R., Mills, G.A., Dominiak, E., Svensson, K., Knutsson, J., Morrison, G., 2005. Passive sampling techniques for monitoring pollutants in water. TrAC Trends Anal Chem 24 (10), 845–868. https://doi.org/10.1016/j.trac.2005.06.006.

[3] Miège, C., Mazzella, N., Allan, I., Dulio, V., Smedes, F., Tixier, C., Vermeirssen, E., Brant, J., O'Toole, S., Budzinski, H., Ghestem, J.-P., Staub, P.-F., Lardy-Fontan, S., Gonzalez, J.-L., Coquery, M., Vrana, B., 2015. Position paper on passive sampling techniques for the monitoring of contaminants in the aquatic environment – achievements to date and perspectives. Trends Environ Anal Chem 8, 20–26. https://doi.org/10.1016/j.teac.2015.07.001.

[4] Charriau, A., Lissalde, S., Poulier, G., Mazzella, N., Buzier, R., Guibaud, G., 2016. Overview of the Chemcatcher® for the passive sampling of various pollutants in aquatic environments part a: principles, calibration, preparation and analysis of the sampler. Talanta 148, 556–571. https://doi.org/10.1016/j.talanta.2015.06.064.

[5] Kingston, J.K., Greenwood, R., Mills, G.A., Morrison, G.M., Björklund Persson, L., 2000. Development of a novel passive sampling system for the time-averaged measurement of a range of organic pollutants in aquatic environments. J Environ Monit 2 (5), 487–495. https://doi.org/10.1039/b003532g.

[6] Booij, K., 2021. Passive sampler exchange kinetics in large and small water volumes under mixed rate control by sorbent and water boundary layer. Environ Toxicol Chem 40 (5), 1241–1254. https://doi.org/10.1002/etc.4989.

[7] Endo, S., Matsuura, Y., Vermeirssen, E., 2019. Mechanistic model describing the uptake of chemicals by aquatic integrative samplers: comparison to data and implications for improved sampler configurations. Environ Sci Technol 53, 1482–1489.

[8] Harman, C., Allan, I.J., Vermeirssen, E.L.M., 2012. Calibration and use of the polar organic chemical integrative sampler—a critical review. Environ Toxicol Chem 31 (12), 2724–2738. https://doi.org/10.1002/etc.2011.

[9] Mutzner, L., Vermeirssen, E.L.M., Mangold, S., Maurer, M., Scheidegger, A., Singer, H., Booij, K., Ort, C., 2019. Passive samplers to quantify micropollutants in sewer overflows: accumulation behaviour and field validation for short pollution events. Water Res 160, 350–360. https://doi.org/10.1016/j.watres.2019.04.012.

[10] Vermeirssen, E.L.M., Asmin, J., Escher, B.I., Kwon, J.-H., Steimen, I., Hollender, J., 2008. The role of hydrodynamics, matrix and sampling duration in passive sampling of polar compounds with empore™ SDB-RPS disks. J Environ Monit 10 (1), 119–128. https://doi.org/10.1039/B710790K.

[11] Gale, R.W., 1998. Three-compartment model for contaminant accumulation by semipermeable membrane devices. Environ Sci Technol 32 (15), 2292–2300. https://doi.org/10.1021/es970754m.

[12] Salim, F., Górecki, T., 2019. Theory and modelling approaches to passive sampling. Environ Sci: Process Impacts 21 (10), 1618–1641. https://doi.org/10.1039/C9EM00215D.

[13] Booij, K., Maarsen, N.L., Theeuwen, M., van Bommel, R., 2017. A method to account for the effect of hydrodynamics on polar organic compound uptake by passive samplers. Environ Toxicol Chem 36 (6), 1517–1524. https://doi.org/10.1002/etc.3700.

[14] Fauvelle, V., Kaserzon, S.L., Montero, N., Lissalde, S., Allan, I.J., Mills, G., Mazzella, N., Mueller, J.F., Booij, K., 2017. Dealing with flow effects on the uptake of polar compounds by passive samplers. Environ Sci Technol 51 (5), 2536–2537. https://doi.org/10.1021/acs.est.7b00558.

[15] Glanzmann, V., Reymond, N., Weyermann, C., Estoppey, N., 2023. An improved chemcatcher-based method for the integrative passive sampling of 44 hydrophilic micropollutants in surface water – Part A: calibration under four controlled hydrodynamic conditions. Sci Total Environ 871, 162037.

[16] Reymond, N., Glanzmann, V., Plagellat, C., Weyermann, C., Estoppey, N., 2023. An improved chemcatcher-based method for the integrative passive sampling of 44 hydrophilic micropollutants in surface water – Part B: field implementation and comparison with automated active sampling. Sci Total Environ 871, 161937.

[17] Estoppey, N., Mathieu, J., Gascon Diez, E., Sapin, E., Delémont, O., Esseiva, P., de Alencastro, L.F., Coudret, S., Folly, P., 2019. Monitoring of explosive residues in lake-bottom water using polar organic chemical integrative sampler (POCIS) and chemcatcher: determination of transfer kinetics through polyethersulfone (PES) membrane is crucial. Environ Pollut 252, 767–776. https://doi.org/10.1016/j.envpol.2019.04.087.

[18] Vermeirssen, E.L.M., Dietschweiler, C., Escher, B.I., van der Voet, J., Hollender, J., 2012. Transfer kinetics of polar organic compounds over polyethersulfone membranes in the passive samplers pocis and chemcatcher. Environ Sci Technol 46 (12), 6759–6766. https://doi.org/10.1021/es3007854.

[19] Wang, R., Zou, Y., Luo, J., Jones, K.C., Zhang, H., 2019. Investigating potential limitations of current diffusive gradients in thin films (DGT) samplers for measuring organic chemicals. Anal Chem 91 (20), 12835–12843. https://doi.org/10.1021/acs.analchem.9b02571.

[20] Becker, B., Kochleus, C., Spira, D., Möhlenkamp, C., Bachtin, J., Meinecke, S., Vermeirssen, E.L.M., 2021. Passive sampler phases for pesticides: evaluation of AttractSPE™ SDB-RPS and HLB versus Empore™ SDB-RPS. Environ Sci Pollut Res 28 (9), 11697–11707. https://doi.org/10.1007/s11356-020-12109-9.

[21] Endo, S., Matsuura, Y., 2018. Characterizing sorption and permeation properties of membrane filters used for aquatic integrative passive samplers. Environ Sci Technol 52 (4), 2118–2125. https://doi.org/10.1021/acs.est.7b05144.

[22] Liang, Y., Li, H., Li, S., Chen, S., 2023. Organic diffusive gradients in thin films (o-DGT) for determining environmental behaviors of antibiotics: a review. J Hazard Mater 459, 132279. https://doi.org/10.1016/j.jhazmat.2023.132279.

[23] Challis, J.K., Hanson, M.L., Wong, C.S., 2016. Development and calibration of an organic-diffusive gradients in thin films aquatic passive sampler for a diverse suite of polar organic contaminants. Anal Chem 88 (21), 10583–10591. https://doi.org/10.1021/acs.analchem.6b02749.

[24] Guibal, R., Buzier, R., Charriau, A., Lissalde, S., Guibaud, G., 2017. Passive sampling of anionic pesticides using the diffusive gradients in thin films technique (DGT). Anal Chim Acta 966, 1–10. https://doi.org/10.1016/j.aca.2017.02.007.

[25] Kaserzon, S.L., Vijayasarathy, S., Bräunig, J., Mueller, L., Hawker, D.W., Thomas, K.V., Mueller, J.F., 2019. Calibration and validation of a novel passive sampling device for the time integrative monitoring of per- and polyfluoroalkyl substances (PFASs) and precursors in contaminated groundwater. J Hazard Mater 366, 423–431. https://doi.org/10.1016/j.jhazmat.2018.12.010.

[26] Belles, A., Alary, C., Aminot, Y., Readman, J.W., Franke, C., 2017. Calibration and response of an agarose gel based passive sampler to record short pulses of aquatic organic pollutants. Talanta 165, 1–9. https://doi.org/10.1016/j.talanta.2016.12.010.

[27] Fialová, P., Šverclová, K., Grabicová, K., Grabic, R., Švecová, H., Nováková, P., Vrana, B., 2024. Performance comparison of three passive samplers for monitoring of polar organic contaminants in treated municipal wastewater. Sci Total Environ 908, 168153. https://doi.org/10.1016/j.scitotenv.2023.168153.

[28] Martins de Barros, R., Rougerie, J., Ballion, T., Buzier, R., Simon, S., Guibal, R., Lissalde, S., Guibaud, G., 2022. Sensitivity improvement of O-DGT for organic micropollutants monitoring in waters: application to neutral pesticides. Talanta Open 6, 100123. https://doi.org/10.1016/j.talo.2022.100123.

[29] Urík, J., Vrana, B., 2019. An improved design of a passive sampler for polar organic compounds based on diffusion in agarose hydrogel. Environ Sci Pollut Res 26 (15), 15273–15284. https://doi.org/10.1007/s11356-019-04843-6.

[30] Yang, Y., Liu, S., Wang, R., Li, C., Tang, J., Chen, T., Ying, G.-G., Chen, C.-E., 2022. Diffusive gradients in thin films (DGT) probe for effectively sampling of per- and polyfluoroalkyl substances in waters and sediments. J Environ Sci 121, 90–97. https://doi.org/10.1016/j.jes.2021.09.003.

[31] Guibal, R., Buzier, R., Lissalde, S., Guibaud, G., 2019. Adaptation of diffusive gradients in thin films technique to sample organic pollutants in the environment: an overview of o-DGT passive samplers. Sci Total Environ 693, 133537. https://doi.org/10.1016/j.scitotenv.2019.07.343.

[32] Zheng, J.-L., Guan, D.-X., Luo, J., Zhang, H., Davison, W., Cui, X.-Y., Wang, L.-H., Ma, L.Q., 2015. Activated charcoal based diffusive gradients in thin films for in situ monitoring of bisphenols in waters. Anal Chem 87 (1), 801–807. https://doi.org/10.1021/ac503814j.

[33] MacKeown, H., Benedetti, B., Scapuzzi, C., Di Carro, M., Magi, E., 2022. A review on polyethersulfone membranes in polar organic chemical integrative samplers: preparation, characterization and innovation. Crit Rev Anal Chem 1–17. https://doi.org/10.1080/10408347.2022.2131374.

[34] Glanzmann, V., Booij, K., Reymond, N., Weyermann, C., Estoppey, N., 2022. Determining the mass transfer coefficient of the water boundary layer at the surface of aquatic integrative passive samplers. Environ Sci Technol 56 (10), 6391–6398. https://doi.org/10.1021/acs.est.1c08088.

[35] Vermeirssen, E.L.M., Bramaz, N., Hollender, J., Singer, H., Escher, B.I., 2009. Passive sampling combined with ecotoxicological and chemical analysis of pharmaceuticals and biocides – evaluation of three chemcatcher™ configurations. Water Res 43 (4), 903–914. https://doi.org/10.1016/j.watres.2008.11.026.

[36] Theory and modeling. In: Huckins, J.N., Booij, K., Petty, J.D. (Eds.), 2006. Monitors of Organic Chemicals in the Environment: Semipermeable Membrane

Devices. Springer US, Boston, MA, pp. 45–85. https://doi.org/10.1007/0–387-35414-X_3.
[37] Schwarzenbach, R.P., Gschwend, P.M., Imboden, D.M., 2016. Environmental Organic Chemistry, 3rd ed.,,. John Wiley & Sons,, Hoboken, USA.
[38] Hayduk, W., Laudie, H., 1974. Prediction of diffusion coefficients for nonelectrolytes in dilute aqueous solutions. AIChE J 20 (3), 611–615. https://doi.org/10.1002/aic.690200329.
[39] León y León, C.A., 1998. New perspectives in mercury porosimetry. Adv Colloid Interface Sci 76–77, 341–372. https://doi.org/10.1016/S0001-8686(98)00052-9.
[40] *Microporous Membrane Resistance Measurement*. Passive Sampling of Organic Compounds /PaSOC. ⟨https://pasoc.eu/microporous-membrane-resistance/⟩ (accessed 2023–07-31).
[41] Booij, K., Chen, S., Trask, J.R., 2020. POCIS calibration for organic compound sampling in small headwater streams. Environ Toxicol Chem 39 (7), 1334–1342. https://doi.org/10.1002/etc.4731.
[42] Booij, K., Chen, S., 2018. Review of atrazine sampling by polar organic chemical integrative samplers and chemcatcher. Environ Toxicol Chem 37 (7), 1786–1798. https://doi.org/10.1002/etc.4160.
[43] Lissalde, S., Charriau, A., Poulier, G., Mazzella, N., Buzier, R., Guibaud, G., 2016. Overview of the Chemcatcher® for the passive sampling of various pollutants in aquatic environments part B: field handling and environmental applications for the monitoring of pollutants and their biological effects. Talanta 148, 572–582. https://doi.org/10.1016/j.talanta.2015.06.076.
[44] Kaserzon, S.L., Hawker, D., Kennedy, K., Bartkow, M., Carter, S., Booij, K., Mueller, J.F., 2014. Characterisation and comparison of the uptake of ionizable and polar pesticides, pharmaceuticals and personal care products by POCIS and chemcatchers. Environ Sci: Process Impacts 16 (11), 2517–2526. https://doi.org/10.1039/C4EM00392F.
[45] Booij, K., Vrana, B., Huckins, J.N., 2007. Chapter 7 theory, modelling and calibration of passive samplers used in water monitoring. In: Greenwood, R., Mills, G., Vrana, B. (Eds.), Comprehensive Analytical Chemistry. Passive Sampling Techniques in Environmental Monitoring; Elsevier, pp. 141–169. https://doi.org/10.1016/S0166-526X(06)48007-7. Vol. 48.
[46] MacKeown, H., Magi, E., Di Carro, M., Benedetti, B., 2022. Unravelling the role of membrane pore size in polar organic chemical integrative samplers (POCIS) to broaden the polarity range of sampled analytes. Anal Bioanal Chem 414 (5), 1963–1972. https://doi.org/10.1007/s00216-021-03832-4.
[47] O'Brien, D., Bartkow, M., Mueller, J.F., 2011. Determination of deployment specific chemical uptake rates for SDB-RPD empore disk using a passive flow monitor (PFM). Chemosphere 83 (9), 1290–1295. https://doi.org/10.1016/j.chemosphere.2011.02.089.
[48] Fialová, P., Grabic, R., Grabicová, K., Nováková, P., Švecová, H., Kaserzon, S., Thompson, K., Vrana, B., 2023. Performance evaluation of a diffusive hydrogel-based passive sampler for monitoring of polar organic compounds in wastewater. Sci Total Environ 864, 161071. https://doi.org/10.1016/j.scitotenv.2022.161071.
[49] Chen, C.-E., Zhang, H., Jones, K.C., 2012. A novel passive water sampler for in situ sampling of antibiotics. J Environ Monit 14 (6), 1523–1530. https://doi.org/10.1039/C2EM30091E.